NeuroImage 59 (2012) 1098–1105

Contents lists available at SciVerse ScienceDirect

NeuroImage

journal homepage: www.elsevier.com/locate/ynimg

Microstructural white matter abnormalities in type 2 diabetes mellitus: A diffusion tensor imaging study

Jung-Lung Hsu [a,b,c], Yen-Ling Chen [d], Jyu-Gang Leu [e], Fu-Shan Jaw [a], Cheng-Hui Lee [f], Yuh-Feng Tsai [f], Chien-Yeh Hsu [c], Chyi-Huey Bai [g,h,*], Alexander Leemans [i]

[a] Institute of Biomedical Engineering, National Taiwan University, Taipei, Taiwan
[b] Department of Neurology, Shin Kong Wu Ho-Su Memorial Hospital, Taipei, Taiwan
[c] Graduate Institute of Biomedical Informatics, College of Medical Science and Technology, Taipei Medical University, Taipei, Taiwan
[d] Division of Endocrinology, Department of Internal Medicine, Shin Kong Wu Ho-Su Memorial Hospital, Taipei, Taiwan
[e] College of Medicine, Fu Jen Catholic University, Taipei, Taiwan
[f] Department of Radiology, Shin Kong Wu Ho-Su Memorial Hospital, Taipei, Taiwan
[g] Central Laboratory, Shin Kong Wu Ho-Su Memorial Hospital, Taipei, Taiwan
[h] Department of Public Health, College of Medicine, Taipei Medical University, Taipei, Taiwan
[i] Image Sciences Institute, University Medical Center Utrecht, Utrecht, The Netherlands

ARTICLE INFO

Article history:
Received 23 March 2011
Revised 5 September 2011
Accepted 15 September 2011
Available online 24 September 2011

ABSTRACT

This study investigated whether diffusion tensor imaging (DTI) could identify potential abnormalities in type 2 diabetes mellitus (T2DM) patients without cognitive complaints compared to healthy controls. In addition, the existence of associations between diffusion measures and clinical parameters was examined. Forty T2DM patients and 97 non-diabetic controls completed a clinical and biochemistry examination. Structural MRI scans (DTI, T1, T2, FLAIR) were subsequently acquired with a 1.5 Tesla scanner. In addition to a global DTI analysis, voxel-based analysis was performed on the fractional anisotropy (FA), mean diffusivity (MD), and axial (AD) and transverse (TD) diffusivity maps to investigate regions that exhibit (i) WM differences between patients and controls; and (ii) associations between clinical measurements and these DTI indices. There were no significant differences in age, gender, and WM hyperintensity scores derived by the conventional MRI scans between controls and T2DM patients. For the T2DM patients, however, the MD of the brain parenchyma was significantly increased compared to controls and was positively correlated with disease duration. The voxel based analyses revealed (i) a significantly decreased FA in the bilateral frontal WM compared to controls which was mainly caused by an increased TD and not a decreased AD within these regions; (ii) a significant association between disease duration and microstructural properties in several brain regions including bilateral cerebellum, temporal lobe WM, right caudate, bilateral cingulate gyrus, pons, and parahippocampal gyrus. Our findings indicate that microstructural WM abnormalities and associations with clinical measurements can be detected with DTI in T2DM patients.

Introduction

Diabetes mellitus (DM) is a common metabolic disease characterized by hyperglycemia due to the insufficient availability of, or insensitivity to, insulin. Diabetes is typically associated with structural brain abnormalities and an increased risk for stroke (Folsom et al., 1999), lacunar infarctions (Kobayashi et al., 1997), silent stroke events (Eguchi et al., 2003), and gray matter atrophy (Manschot et al., 2006; Musen et al., 2006). While the relationship between white matter (WM) hyperintensities and diabetes is still controversial, a recent systematic review on diabetes and brain imaging concluded that there is convincing evidence for an association between diabetes and cerebral atrophy and lacunar infarctions (van Harten et al., 2006). It was stated, however, that it is still unclear whether or not type 2 diabetes mellitus (T2DM) is associated with WM hyperintensities as observed with magnetic resonance imaging (MRI). With nine of the 27 WM lesion studies included in their meta-analysis, no association between diabetes and WM hyperintensities was observed in the "vascular cohorts". By contrast, for the "outpatient cohorts", there appeared to be a modest association between diabetes and WM hyperintensities. This uncertainty could be partly due to the insufficient sensitivity of conventional MRI modalities (e.g., T1 and T2 maps) to detect subtle brain WM changes or to assess the severity of WM hyperintensities. In the review paper of van Harten et al., 2006, it was also suggested that diffusion tensor imaging (DTI) could be a promising technique for the investigation of WM properties in diabetes patients.

* Corresponding author at: Department of Public Health, College of Medicine, Taipei Medical University, Taipei, Taiwan.
E-mail address: baich@ms4.hinet.net (C.-H. Bai).

1053-8119/$ – see front matter © 2011 Elsevier Inc. All rights reserved.
doi:10.1016/j.neuroimage.2011.09.041

DTI is a unique technique for assessing WM structural properties based on the three-dimensional anisotropic Gaussian diffusion of water molecules (Basser et al., 1994). With DTI the directionality and magnitude of random water movement in tissue can be estimated yielding several quantitative measures, such as the three principle diffusivities (i.e., the eigenvalues of the diffusion tensor: $\lambda_1 > \lambda_2 > \lambda_3$), mean diffusivity ($MD = [\lambda_1 + \lambda_2 + \lambda_3]/3$), transverse diffusivity ($TD = [\lambda_2 + \lambda_3]/2$), axial diffusivity ($AD = \lambda_1$), and the degree of diffusion anisotropy (e.g., the fractional anisotropy: FA) (Pierpaoli and Basser, 1996). Without barriers, water molecules move uniformly in all directions, which results in isotropic diffusion. By contrast, in the presence of barriers, such as cell membranes, nerve fibers, or myelin sheets, the diffusion rate is typically larger in one direction than in another, which is then referred to as anisotropic diffusion (Beaulieu, 2002). Being quantitative in nature, these DTI based measures have been shown to be more sensitive to tissue abnormalities than the typical visual evaluation of WM hyperintensities observed in conventional MRI data (Della Nave et al., 2007; Van Hecke et al., 2008a). To date, DTI studies have revealed WM alterations through measurements of decreased FA and/or increased MD in a variety of conditions, including aging (Hsu et al., 2008; Sullivan and Pfefferbaum, 2007; Van Hecke et al., 2008a), multiple sclerosis (Patel et al., 2007), schizophrenia (e.g., Carpenter et al., 2008), traumatic brain injury (e.g., Caeyenberghs et al., 2010a, 2010b), amyotrophic lateral sclerosis (e.g., Sage et al., 2009) and Alzheimer's disease (e.g., Stahl et al., 2007). For an in-depth discussion of DTI, the interested reader is referred to a recent review of Tournier et al. (2011).

Only a few studies have been published that use DTI to investigate WM properties in DM patients. Kodl et al. (2008) demonstrated that DTI can detect microstructural WM abnormalities in subjects with long-standing type 1 DM and they showed that poor performance on selected neurocognitive tests correlated with reduced WM FA. More recently, another study examined the emotional and declarative memory impairment and associated WM microstructural properties in 24 middle-aged and elderly patients *with* T2DM but *without* any obvious vascular pathology or psychiatric disorder (Yau et al., 2009). Their findings suggest that T2DM patients show diffuse and predominantly frontal and temporal WM microstructural abnormalities, with extensive involvement of the temporal stem. Also the FA of the temporal stem was found to be associated with immediate memory performance.

In this work, we studied the WM microstructural organization in a well-controlled and large ($n = 40$) cohort of non-hypertensive T2DM patients who do *not* exhibit significant cognitive deficits. In particular, we investigated whether DTI is able to detect differences in diffusion properties (i.e., FA, MD, TD, and AD) between these patients and healthy controls *even* when the conventional MRI data of the T2DM patients do not show any significant abnormalities. In addition, we performed a battery of medical tests to examine potential relationships between the DTI indices and clinical parameters. Our results demonstrate that, compared with age-matched non-diabetes controls, T2DM patients show several regions with abnormal diffusion values reflecting DM related changes in microstructural tissue organization. To the best of our knowledge, this is the largest DTI based T2DM study to date (40 patients vs. 97 controls) and the first one that also investigates both regional and global diffusivity measures, including AD and TD, providing a more detailed picture of the underlying microstructural tissue organization in T2DM patients.

Methods

Subjects

Forty-two middle-aged T2DM patients (27M/15F) and 100 non-diabetic non-hypertensive controls (54M/46F) were examined by a collaborating endocrinologist based on the guideline criteria of "The American Diabetes Association: clinical practice recommendations 1996". The patients were selected from our community-based prospective cohort study, which investigates the cardio- and cerebrovascular risk factors in the general population, or were recruited from a general health screening program. The duration of disease was measured from the date of diagnosed T2DM to the MRI scanning date. Diabetic subjects were on various oral hypoglycemic agents without any history of insulin treatment and hypoglycemic episode. The control subjects were recruited from the health screening program in the Shin-Kong Wu Ho-Su Memorial Hospital, Taipei, Taiwan.

Both patients and controls received detailed examinations, including physical and bed-side neurological examinations (such as checking the cranial nerves, the motor system, and any cerebellar signs) performed by neurologists, a biochemistry study, a chest X-ray, an electrocardiogram, and an electroencephalogram prior to the data acquisition. All participants who had a history of major neurological diseases, cerebrovascular accidents, psychiatric or serious cardiovascular diseases, or those with manifestations of stroke (demonstrated by abnormal bedside neurological examination) were excluded. In addition, subjects with significant cognitive deficits, i.e. with cognitive complaints that cause impairment in social or occupational functioning, were not included. Body height and weight were measured by a validated automated device (TBF-22, TANITA Co. Ltd, Japan) from which the body mass index (BMI) was calculated. Blood pressure (BP) was measured with a validated oscillometric automated digital BP device (OMRON HEM-757; Omron Matsusaka Co. Ltd, Japan) after examinees had rested for at least 5 min. Subjects were classified hypertensive and were excluded from this study if they received anti-hypertensive treatment or if they had a BP above the cut-off value (a systolic BP>= 140 mm Hg or a diastolic BP>= 90 mm Hg). The biochemistry tests included the assessment of fasting glucose, glycated hemoglobin (HbA1c), triglycerides, total cholesterol, high-density lipoprotein (HDL), and low-density lipoprotein (LDL). Any MRI scans (see acquisition details below) with structural abnormalities, such as a tumor or stroke, obvious variations (e.g., mega cisterna magna, cavum septum pellucidum), or technical acquisition artifacts were excluded. Additionally, other brain WM properties, as observed on T2-weighted and fluid-attenuated inversion recovery (FLAIR) images, were also rated by one of the authors (JL) using the age-related WM changes (ARWMC) score (Wahlund et al., 2001). Subsequently, all subjects with a regional ARWMC score higher than 1, which corresponds to the beginning confluence of lesions in periventricular WM abnormalities at that location, were also excluded. Summation of all the regional ARWMC scores was performed to construct the total ARWMC score in each individual. In the control group, three subjects were excluded due to white matter hyperintensities in the bilateral parietal lobes and other regions (subject one: total ARWMC = 6; subject two: total ARWMC = 10) and the bilateral frontal lobes (subject three: total ARWMC = 4). In the T2DM group, two subjects were excluded: one subject had white matter hyperintensities in the bilateral frontal and parietal lobes (total ARWMC = 8) and the other one had an asymptomatic dural arteriovenous malformation. There were no data sets with technical acquisition artifacts. The final number of participants included in this study was 137, consisting of 40 T2DM patients (25M/15F) and 97 non-diabetic non-hypertensive controls (54M/43F). A summary of inclusion and exclusion criteria for T2DM patients and control subjects is presented in Table 1. All participants gave their informed consent and the Ethics Committee of the hospital approved the protocol of this study.

MR image acquisition

All participants received whole-brain MRI scans (Siemens, 1.5T Avanto, Erlangen, Germany) within 1 week after the clinical examination. First, trans-axial T2-weighted scans (TR/TE = 4860/98 ms, NEX = 2, voxel size $0.43 \times 0.43 \times 5$ mm^3), FLAIR images (TR/TE = 9790/106 ms, inversion time 2500 ms, NEX = 2, voxel size $0.45 \times 0.45 \times 5$ mm^3), and high-resolution sagittal T1-weighted images (TR/TE = 8.8/4.7 ms, NEX = 1,

Table 1
Summary table of inclusion and exclusion criteria for T2DM patients and controls.

Criteria	T2DM patients and controls
Inclusion	Age: 40–70 years old.
	T2DM criteria using ADA criteria 1996. Patient did not have any history of insulin treatment or hypoglycemic episode.
	No history of major neurological diseases, cerebrovascular accidents, psychiatric or serious cardiovascular diseases, or those with manifestations of stroke demonstrated by abnormal bedside neurological examination.
	No cognitive complaints that cause impairment in social or occupational functioning.
	No history of anti-hypertensive treatment or if they had a BP above the cut-off value (a systolic BP>= 140 mm Hg or a diastolic BP>= 90 mm Hg).
Exclusion	Any T1 MRI scans with structural abnormalities, such as a tumor or stroke, obvious variations (e.g., mega cisterna magna, cavum septum pellucidum), or technical acquisition artifacts.
	WM abnormalities: brain WM properties, as observed on T2-weighted and FLAIR images, rated by one of the authors (JL) using the age-related WM changes (ARWMC) score. A regional ARWMC score higher than 1, which corresponds to the beginning confluence of lesions in periventricular WM abnormalities at that location.

voxel size $1.0\times1.0\times1.0$ mm^3) were acquired. Secondly, single-shot spin-echo echo-planar whole-brain DTI scans were acquired axially with a fat suppression sequence (TR/TE = 7600/82 ms, 3 mm slice thickness without gap, slice acquisition matrix = 128×128 with FOV = 256×256 mm^2, 6/8 partial Fourier, NEX = 2, 55 slices, 12 gradient directions with b-value = 1000 s/mm^2, and one b = 0 s/mm^2 image) (Jones and Leemans, 2011).

Image processing

The DTI based pre-processing steps performed in this work have been described previously in detail (Hsu et al., 2008, 2010). In summary, the following steps were taken:

(a) All DTI data sets were corrected for eddy current induced geometric distortions and subject motion (Leemans and Jones, 2009).
(b) The diffusion tensor model was fitted to the data with *ExploreDTI* (Leemans et al., 2009) using a non-linear regression method. The diffusion measures (FA, MD, RD, and AD) were subsequently computed (Pierpaoli and Basser, 1996).
(c) A population-based DTI atlas in MNI space was constructed (Hsu et al., 2010; Van Hecke et al., 2008b) to drive the tensor based affine (Leemans et al., 2005) and non-affine (Van Hecke et al., 2007) coregistration techniques. At the final transformation step, the "preservation of principal direction" strategy was applied to reorient the diffusion tensor (Alexander et al., 2001b). This coregistration approach has already been applied successfully in a wide range of applications, where adjusting for morphological inter-subject (and inter-group) differences, such as, for instance, ventricle size, is considered to be necessary (Van Hecke et al., 2010; Sage et al., 2009; Verhoeven et al., 2010).

Global analysis

The intracranial brain was extracted from the b = 0 s/mm^2 image with BET2, the brain extraction tool from FSL (http://www.fmrib.ox.ac.uk/fsl/) (Smith, 2002). The brain was further subdivided into its cerebrospinal fluid (CSF) regions and brain tissue (combined GM and WM) by segmenting all CSF voxels using an automated gray-level thresholding method, performed on the MD map (Otsu, 1979). For each subject, the mean FA, MD, AD, and TD of brain tissue were calculated. Potential group differences were examined with a two-way ANOVA (controlling for age effects). To investigate the relationship between the clinical parameters and the global DTI indices in the patient group, we used the linear regression model with age as a covariate.

Voxel based analysis

In addition to the global analysis, a whole-brain voxel-based analysis was performed using the statistical non-parametric mapping (SnPM) toolbox to search for brain regions with significant differences in FA and MD between the diabetic patients and non-diabetic controls (Ashburner and Friston, 2000). In summary, the general linear model in SnPM was applied to construct pseudo t-statistic images, which were then assessed for significance using a standard non-parametric multiple comparisons procedure based on randomization/permutation testing (Nichols and Holmes, 2002). Then, a two-sample *T*-test with age as a covariate was applied to assess potential differences. No spatial smoothing was performed on the normalized DTI images prior to the statistical analysis to prevent the introduction of any filter bias (Van Hecke et al., 2010). The resulting voxels constituted pseudo t-statistic images and their thresholds were subsequently defined at the threshold: t-value>= 2 (corresponding false discovery rate $p<0.03$ level). Cluster sizes larger than 50 voxels were considered significant after correction for multiple independent comparisons. To study the potential FA (or MD) differences between T2DM patients and healthy controls in more detail, an image mask from the regions with significant FA (or MD) differences was created and applied to the each individual's AD and TD image. Potential group differences in mean AD and TD, controlled for age effects, were investigated with a two-way ANOVA. Subsequently, to explore the relationship between the clinical parameter (s)-of-interest (as determined by the outcome of the global analyses) and the FA and MD images, the multiple regression model from the SPM toolbox was applied (Ashburner and Friston, 2000) with age as covariate-not-of-interest (significance level and cluster size as defined above). Finally, volumetric estimates of GM, WM and CSF were calculated from the T1 images using the Unified Segmentation (US) approach, as implemented in SPM8 (Ashburner and Friston, 2005). Total intracranial volume (TIV) was defined as the summation of GM, WM and CSF volumes. Potential volumetric group differences for each of these components, controlled for age effects, were investigated with a two-way ANOVA. We also investigated the group differences for each fraction of the brain components (defined by GM/TIV∗100%, WM/TIV∗100% and CSF/TIV∗100%), controlled for age effects using a two-way ANOVA

Results

Descriptive statistics of clinical measures

Clinical and demographic characteristics of the T2DM patients and the age-matched healthy controls are shown in Table 2. There is no significant difference in age, gender, total cholesterol, LDL, and total ARWMC scores between both groups (assessed with two-tailed independent sample t-tests and Chi-square tests). However, diabetic patients have higher levels of BMI, systolic and diastolic BP, fasting glucose, HbA1c, and triglyceride; and lower HDL levels than controls. As shown in Table 3, for diabetic patients, age was positively correlated with disease duration, HDL, and the total ARWMC score; and negatively associated with triglyceride and BMI (using Pearson's correlation method). In addition, disease duration did not correlate with LDL. Furthermore, there are significant negative correlations between the mean MD, AD, and TD measures on the one hand and triglycerides on the other hand. Finally, the MD and TD are correlated with BMI as well.

Global analysis

Table 2 shows the mean and standard deviation (SD) of the global DTI indices within brain parenchyma for both groups. Here, the MD was significantly different between groups, which can be mainly attributed to the significantly increased TD in T2DM patients. With a 2-way ANOVA (correcting for age effects), the significant correlation that could be observed between the DTI measures and the clinical parameters was between disease duration and the MD (Fig. 1). Investigating the observed increase of the MD with disease duration in more detail revealed that both the associated AD and TD are highly correlated with disease duration (whole model age-adjusted p-values for AD and TD are 0.0021 and 0.0034, respectively) (Fig. 1).

Regional (voxel based) inter-group analysis

Two clusters of a significantly lower regional FA were found in the T2DM group compared to the controls (10^4 permutations and using age as a covariate-not-of-interest) and were distributed on the bilateral frontal WM area (Fig. 2(A)). Further inspection revealed that these FA decreases in T2DM patients were mainly caused by a significant increase in the corresponding TD (T2DM vs. controls: $[66.8 \pm 5.4] \times 10^{-5}$ mm^2/s vs. $[62.7 \pm 5.4] \times 10^{-5}$ mm^2/s with age-adjusted group difference $p<0.001$), since there was no significant difference in AD (T2DM vs. controls: $[87.6 \pm 4.3] \times 10^{-5}$ mm^2/s vs. $[87.4 \pm 4.3] \times 10^{-5}$ mm^2/s with age-adjusted group difference $p=0.81$). No significant regional increases in FA were observed.

For the MD analysis, the patient group showed twelve clusters with a significantly higher MD compared to the healthy subjects (while correcting for age effects). The distribution of the regions included the bilateral anterior and posterior lobes of the cerebellum, bilateral temporal lobe WM, the left parahippocampal gyrus, the left fusiform gyrus, and the left cuneus WM (Fig. 2(B)). Post-hoc analysis showed significant increases in both the associated TD and AD for T2DM patients (for TD, T2DM vs. controls: $[67.1 \pm 4.0] \times 10^{-5}$ mm^2/s vs. $[62.3 \pm 3.0] \times 10^{-5}$ mm^2/s with age-adjusted group difference $p<0.001$, and for AD, T2DM vs. controls: $[96.8 \pm 4.8] \times 10^{-5}$ mm^2/s vs. $[91.9 \pm 3.9] \times 10^{-5}$ mm^2/s with age-adjusted group difference $p<0.001$). There were no significant regional decreases in MD in the T2DM group.

Table 2
Demographic data and global DTI indices of brain parenchyma for T2DM patients and healthy controls.

	T2DM patients	Healthy controls	p-value
N	40	97	
Age (years)	56.8 ± 5.5	56.2 ± 4.7	0.40
Gender (M/F)	25/15	54/43	0.46
Diabetes duration (years)	5.1 ± 4.7	N/A	N/A
BMI (kg/m2)	25.3 ± 3.6	23.6 ± 2.9	0.0139
Systolic BP (mm Hg)	121.4 ± 11.4	113.6 ± 13.3	0.00043
Diastolic BP (mm Hg)	73.5 ± 6.6	69.5 ± 9.7	0.016
Glucose (mmol/l)	141.4 ± 44.3	90.3 ± 10.1	<0.0001
HbA1c (%)	7.7 ± 1.7	5.5 ± 0.3	<0.0001
Triglycerides (mg/dl)	158.4 ± 98.6	121.9 ± 63.4	0.0379
Cholesterol	198.1 ± 39.1	211.7 ± 37.2	0.06
HDL (mmol/l)	46.6 ± 11.2	61.9 ± 20.8	<0.001
LDL (mmol/l)	138.9 ± 33.9	140.3 ± 38.9	0.83
Total ARWMC score	0.4 ± 0.7	0.4 ± 0.8	0.88
FA	0.251 ± 0.008	0.255 ± 0.009	0.07
MD ($\times 10^{-5}$ mm^2/s)	81.8 ± 3.5	80.3 ± 3.3	0.03
AD ($\times 10^{-5}$ mm^2/s)	102.4 ± 4.4	100.8 ± 4.4	0.07
TD ($\times 10^{-5}$ mm^2/s)	71.5 ± 3.1	70.0 ± 2.9	0.02

Data values are expressed in means ± SD (or in frequency).
BMI: body mass index; BP: blood pressure; HbA1c: glycated hemoglobin; HDL: high-density lipoprotein; LDL: low-density lipoprotein; ARWMC: age-related WM changes; FA: fractional anisotropy; MD: mean diffusivity; AD: axial diffusivity; TD: transverse diffusivity.
The p-values for the FA, DM, AD, and TD were age-adjusted (two-way ANOVA).

Regional (voxel based) association analysis

As disease duration was the only clinical parameter that showed significance in the exploratory global analysis, it was used as the covariate-of-interest in the voxel based association analysis. Three clusters in the area of the bilateral posterior cerebellar lobes and the right frontal lobe WM showed a significant negative correlation between disease duration and FA while correcting for age effects (Table 4; bottom row Fig. 3 (A)). In addition, four clusters with a significant positive correlation were found in the left brainstem, the right lentiform nucleus, and the bilateral frontal lobe WM (Table 4; top row Fig. 3(A)). For the brain regions that showed a negative correlation between FA and disease duration, both AD and TD showed a significant positive ($p=0.029$ for AD and $p<0.0001$ for TD) correlation with disease duration. By contrast, for brain regions showing a positive correlation between FA and disease duration, AD showed a significantly positive ($p<0.0001$), but TD a significantly negative ($p=0.0006$) correlation with the disease duration.

Performing the association analysis between disease duration and MD (again, using age as covariate-not-of-interest) resulted in thirty clusters with a significant positive correlation (Fig. 3(B)). The largest 10 clusters are summarized in Table 5. The distribution of these areas included the right caudate, the bilateral cingulate WM gyrus, the bilateral anterior lobes of the cerebellum, the right superior temporal WM gyrus, and the pons (Fig. 3(B)).Within these significant regions, both the AD and TD showed significant positive (both $p<0.0001$) correlations with disease duration. No significant negative correlations between disease duration and MD were found.

The GM, WM and CSF volumes, which were estimated with the US method from SPM, did not show any significant group differences (2-way ANOVA, corrected for age effects). In summary, the GM, WM, and CSF volumes were T2DM: 604 ± 63 ml vs. controls: 616 ± 62 ml ($p=0.37$), T2DM: 457 ± 51 ml vs. controls: 472 ± 61 ml ($p=0.20$), and T2DM: 485 ± 86 ml vs. controls: 472 ± 102 ml ($p=0.47$), respectively. In addition, there was no significant ($p=0.69$) difference in TIV between T2DM (1547 ± 147 ml) and controls (1559 ± 150 ml). There is also no significant group difference in the fraction of each brain component. The GM, WM, and CSF fractions were T2DM: 39.1 ± 3% vs. controls: 39.5 ± 3% ($p=0.41$), T2DM: 29.6 ± 2% vs. controls: 30.3 ± 3% ($p=0.20$), and T2DM: 31.3 ± 4% vs. controls: 30.1 ± 5% ($p=0.19$), respectively.

Discussion

In this investigation, we demonstrated significant differences in the microstructure of brain tissue, as determined by global and voxel based analyses of FA, MD, RD, and AD measures, between T2DM patients and healthy controls. More specifically, we observed a regionally decreased FA in T2DM patients due to a significantly increased TD (with no significant decrease in AD). In addition, for both the global and regional analysis, the observed increase in MD for T2DM patients compared to healthy controls can be mainly attributed to the increased TD. Further analysis revealed significant correlations between disease duration and diffusion metrics in several brain regions. As an example, the most significant association was found with the MD in the left frontal WM. Crucial in these analyses was to incorporate age as a covariate-not-of-interest, as it is a well-known fact that for both healthy and diseased subjects diffusion measures, such as FA and MD, are highly dependent on age (Bastin et al., 2010; Hsu et al., 2008; Lebel et al., 2008; Salat et al., 2005; Van Hecke et al., 2008a).

Table 3
Pearson correlation matrix of the clinical measures in T2DM patients.

	Disease duration	BMI	Glucose	HbA1c	Triglycerides	Cholesterol	HDL	LDL	Total ARWMC	FA	MD	AD	TD
Age	0.3606*	−0.4554*	0.0016	−0.1857	−0.5367*	0.0134	0.3445*	0.1538	0.3173*	−0.0411	0.3671*	0.3482*	0.3708*
Disease duration		−0.2041	0.2636	0.1037	−0.0445	−0.1315	0.1755	−0.3852*	0.2105	−0.1089	0.4927*	0.4784*	0.4898*
BMI			−0.1417	−0.0017	0.5599*	−0.0302	−0.2815	−0.0753	−0.1888	0.2407	−0.3313*	−0.2898	−0.3520*
Glucose				0.7013*	0.2708	0.2843	0.0808	−0.0838	−0.1493	−0.1710	0.2182	0.1869	0.2346
HbA1c					0.2632	0.2313	0.0093	0.0374	−0.1926	−0.0290	0.1788	0.1692	0.1809
Triglycerides						0.2626	−0.4095*	0.0727	−0.1512	0.1685	−0.4597*	−0.4335*	−0.4662*
Cholesterol							0.1984	0.6917*	−0.3382*	−0.0396	−0.0807	−0.0928	−0.0699
HDL								−0.0468	−0.0803	−0.2881	0.1653	0.1079	0.2019
LDL									−0.1517	−0.1071	−0.1838	−0.2145	−0.1572
Total ARWMC										−0.0397	−0.0864	−0.0978	−0.0759
FA											−0.1969	−0.0009	−0.3312*
MD												0.9784*	0.9892*
AD													0.9375*

Data values represent the Pearson correlation coefficient.
For abbreviations, see Table 1.
* $P<0.05$ (not corrected for multiple hypothesis testing).

In this study, the conventional MRI scans, such as the T2-weighted or the FLAIR images, did not reveal any significant WM intensity abnormalities or volumetric differences between T2DM patients and healthy controls. In this context, the relationship between WM hyperintensities (number/volume) observed in these conventional images and T2DM remains controversial. For instance, using a volumetric method based on inversion recovery and FLAIR images, one study showed 56% larger WM hyperintensity volumes in T2DM patients than in controls (Jongen et al., 2007). Another study investigating FLAIR images, showed no significant difference in total WM hyperintensity volume, except in lesion volume (Novak et al., 2006). The few DTI based diabetes studies that have appeared in recent literature, however, seem to be more in agreement with each other. Both Kodl et al. and Yau et al., for instance, showed significantly lower FA

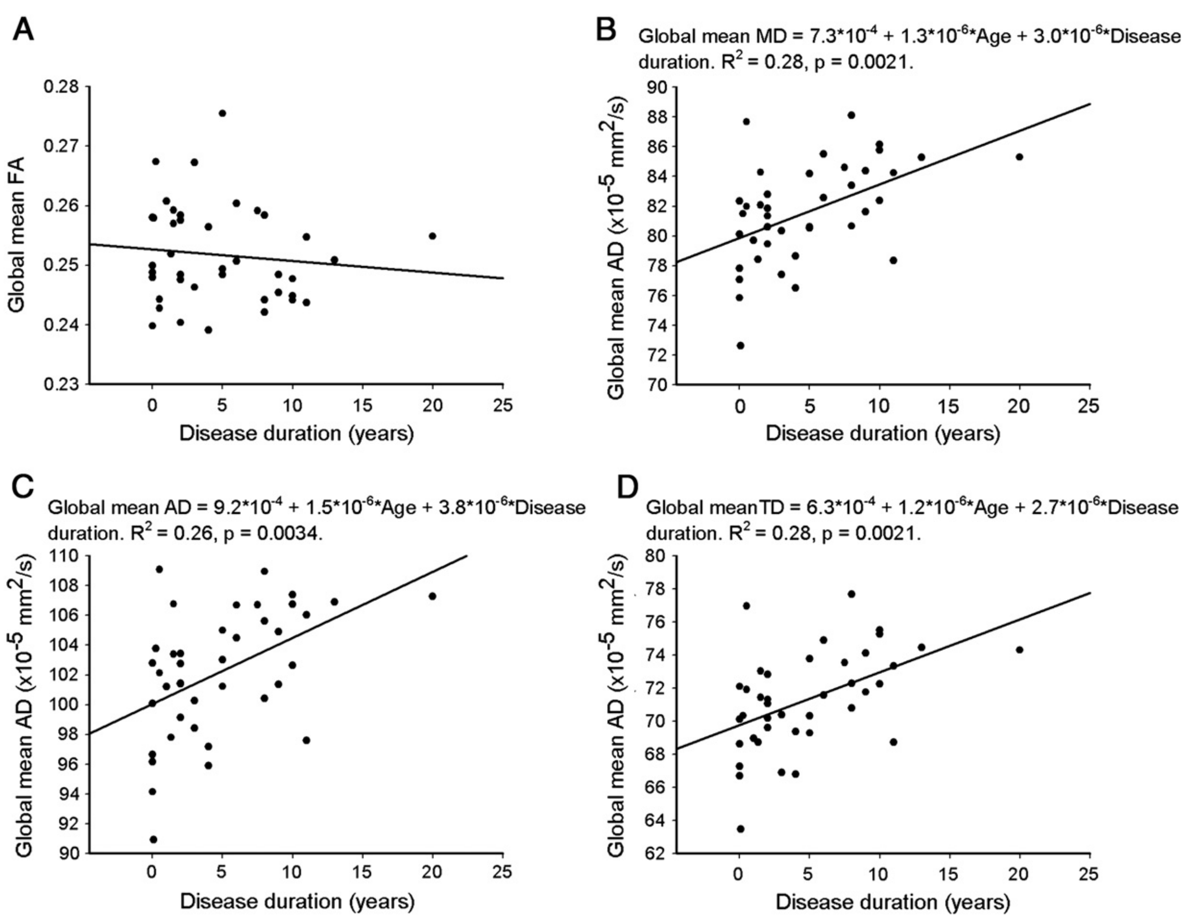

Fig. 1. Effect of disease duration on the global DTI parameters FA (A), MD (B), AD (C), and TD (D) using age as covariate. Only the FA did not show a significant correlation with disease duration. The solid line represents the age-adjusted regression line between disease duration and global MD in brain parenchyma. The trend slopes for disease duration and age, and the *p* value for regression line are also indicated for the significant correlations. FA: fractional anisotropy; MD: mean diffusivity; AD: axial diffusivity; TD: transverse diffusivity.

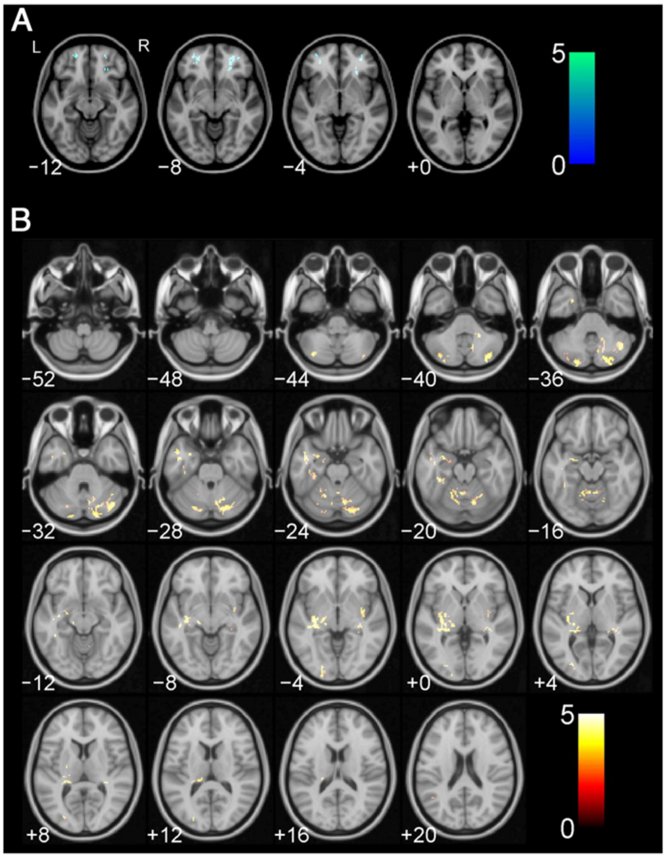

Fig. 2. Maps showing significant inter-group differences in FA (A) and MD (B). (A) Voxel-based significance maps of the decreased FA in diabetic patients, as computed by SnPM pseudo *t*-tests at the voxel level. The 'cold' color scale represents the pseudo *t*-value significance for the FA decreases. (B) Voxel-based significance maps of the increased MD in diabetic patients, as computed by SnPM pseudo *t*-tests at the voxel level. The 'hot' color scale represents the pseudo *t*-value significance for the MD increases. The number indicates the *z*-axis coordinate in the MNI space (unit in mm). R: right side, L: left side, FA: fractional anisotropy; MD: mean diffusivity.

values in several brain regions, including the posterior corona radiata and the optic radiation in type 1 DM patients (Kodl et al., 2008) and the frontal and temporal WM in T2DM subjects (Yau et al., 2009). In our study, we also showed a decreased regional FA in the bilateral frontal WM. In contrast to Yau et al., however, we also investigated the diffusivities (MD, AD, TD), which – being independent of the FA – provide a more complete picture of the changes in the underlying microstructural tissue organization in T2DM patients. The decreased FA in the frontal WM in our study, for instance, was driven by the increase in TD and not by an increase in AD, providing more specific information about the pathogenesis of the observed WM changes (Beaulieu, 2002; Pierpaoli et al., 2001; Song et al., 2002). According to a study of Song et al. (2003), changes in AD are more related to axonal injury, whereas the TD may be modulated more directly by myelin alterations. The observed increase in TD, which caused the FA decrease in the frontal WM, therefore suggests that demyelination may be present in T2DM patients. In another result of this work, disease duration was significantly associated with MD but *not* with FA (Fig. 1) — highlighting the relevance of including these diffusivity measures. The regional analysis also demonstrated that many brain areas showed a significant positive correlation between MD and disease duration. Again, in these regions, the AD and TD were positively correlated with disease duration, suggesting that the degree of microstructural alteration in terms of both axonal injury and demyelination could be related to disease duration.

Table 4
Overview voxel-based analysis: summary statistics of the brain regions that showed a significant correlation between disease duration and fractional anisotropy (age included as a covariate-not-of-interest).

Structure name	Cluster voxel number[a]	Peak T value	MNI coordinates of cluster centroid (mm)		
			X	Y	Z
Negative correlate with disease duration					
Cerebellum posterior lobe (L)	291	4.94	−20	−78	−24
Middle frontal gyrus WM (R)	99	3.83	34	2	42
Cerebellum posterior lobe (R)	50	3.74	36	−50	−48
Positive correlate with disease duration					
Brainstem (L)	57	4.64	−10	−26	−14
Lentiform nucleus (R)	114	4.26	18	0	6
Middle frontal gyrus WM (R)	86	3.95	20	14	40
Medial frontal gyrus WM (L)	87	3.82	−14	34	36

MNI: Montreal Neurological Institute; WM: white matter; R: right side; L: left side.
[a] Voxel size: 8 mm^3.

Specifically for diabetes, both glucose toxicity and abnormal insulin metabolism have been suggested to impact the structure of the brain, even to a higher degree than circumscriptive vascular lesions (Biessels et al., 2006). Comparing type 1 diabetes patients with and without retinopathy, a significant change in brain structure was found in the cerebellum (Wessels et al., 2006). In a recent animal study, degenerative changes, such as disarrangement of myelin sheaths, fragmentation of neurofilaments, and oligodendrocyte abnormalities were also detected in the cerebellum of streptozotocin-induced diabetes rats (Hernandez-Fonseca et al., 2009). The increased MD values in T2DM patients observed in this study are located predominantly in the cerebellar area and are, therefore, well-supported by these previous reports.

Potential relationships between clinical parameters (Table 2) and microstructural WM changes have not yet been studied in great detail. In a previous study, Gold et al. (2007) showed a significant negative correlation between hippocampus volume and HbA1c. More recently, Kodl et al. (2008) showed that disease duration of diabetes patients is negatively correlated with the FA of the splenium of the corpus callosum. Investigating both parameters simultaneously, our findings reveal that disease duration, rather than the HbA1c or the fasting glucose, is related to WM abnormalities in T2DM patients. The involved regions included the bilateral cingulate gyrus, the superior temporal gyrus, the pons, and the cerebellum. Note that in a recently published study, disease duration was also found to be an important contributing factor for developing diabetic peripheral neuropathy or cardiovascular autonomic neuropathy in the T2DM patients (Chen et al., 2008; Hsu et al., 2007).

There are several limitations in this study. Disease duration of the T2DM patients is estimated by the patient's history or medical records. Since this estimation could be affected by the patient's awareness and examination time it might not be very accurate. In addition, several oral hypoglycemic agents were taken by these subjects and there is no knowledge about how these various drugs may affect the DTI indices. Although only normotensive T2DM patients were included in this study, their BP was still significantly higher compared to the healthy control group. Since hypertension was recently shown to be associated with a decrease in FA, it is not clear to which degree this modulation may have influenced our results (Burgmans et al., 2010). Although our subjects did not have any significant cognitive complaints, it is unknown to what extent subtle cognitive impairment could still affect the diffusion changes. In this context, Yau et al. (2010) showed that declarative memory impairment could be found in T2DM patients. Furthermore, obese adolescents with T2DM also have been shown to exhibit brain structural changes as revealed by DTI (Yau et al., 2010). The mean BMI index of our T2DM patient group, however, is 25.3 kg/m^2, which is significantly lower than the mean BMI index described in the study of Yau et al. (2010) (mean BMI index is 37.7 kg/m^2). Another limitation is related to the relatively large slice thickness (5 mm) of the T2-weighted

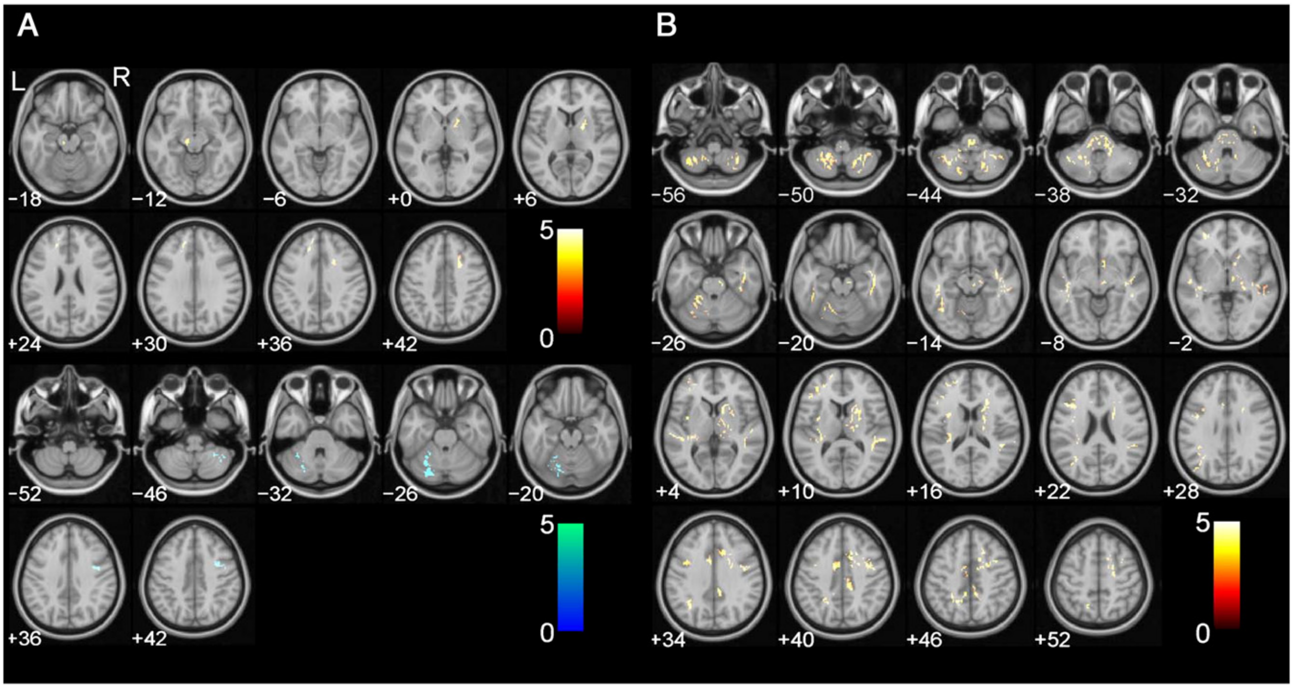

Fig. 3. *T*-value significance maps of the FA (A) and MD (B) associations with disease duration. (A) Voxel-based significance maps of the FA showing positive correlations with the disease duration (with age as a covariate-not-of-interest), as computed by *t*-tests at the voxel level (see bottom row with the 'hot' color map representing the t-statistic values). The top row shows the FA changes that correlated negatively with the disease duration (with the 'cold' color map representing the t-statistic values). (B) Voxel-based significance maps showing a positive correlation between disease duration and the MD (with age as covariate-not-of-interest), as computed by *t*-tests at the voxel level. The number indicates the *z*-axis coordinate in the MNI space (unit in mm). R: right side, L: left side, FA: fractional anisotropy; MD: mean diffusivity.

and the FLAIR images. The total ARWMC scores may be biased toward larger WM lesions, since lesions smaller than 5 mm may not be detected. Finally, it is important to acknowledge the limitations of DTI in terms of specificity. In other words, it is well-known that there are many brain regions with complex fiber architecture (i.e., "crossing fibers") and partial volume effects that may affect diffusivity measures in a non-trivial way (Alexander et al., 2001a; Vos et al., 2011; Wheeler-Kingshott and Cercignani, 2009). As a result, changes in DTI based measures may be hard to interpret in an unambiguous way. Notwithstanding the assumptions and limitations of DTI (e.g., low resolution and inadequacy to resolve multiple fiber orientations), we have shown that it is indeed a promising tool to investigate microstructural WM abnormalities in T2DM patients.

Table 5
Overview voxel-based analysis: summary statistics of the brain regions that showed a significant positive correlation between disease duration and mean diffusivity (age included as a covariate-not-of-interest).

Structure name	Cluster voxel number[a]	Peak T value	MNI coordinates of cluster centroid (mm)		
			X	Y	Z
Inferior frontal gyrus WM (L)	363	5.52	−46	20	18
Cingulate gyrus WM (R)	124	5.12	8	−38	22
Caudate (R)	1139	5.09	14	12	10
Superior temporal gyrus WM (R)	527	5.03	48	−36	12
Cingulate gyrus WM (R)	139	4.90	−10	−2	42
Precuneus (L)	141	4.87	−24	−52	44
Pons WM	1649	4.87	−2	−26	−40
Parietal lobe WM (L)	136	4.58	−32	−60	32
Fusiform gyrus WM (L)	449	4.36	−40	−50	−14
Middle frontal gyrus WM (L)	117	3.95	−30	48	−4

MNI: Montreal Neurological Institute; WM: white matter; R: right side; L: left side.
[a] Voxel size: 8 mm^3.

Author contributions

Jung-Lung Hsu: wrote manuscript, designed analysis, investigated data, performed analyses.
Yen-Ling Chen: investigated data.
Chyi-Huey Bai: contributed to discussion.
Fu-Shan Jaw: contributed to discussion.
Cheng-Hui Lee: investigated data.
Yuh-Feng Tsai: investigated data.
Chien-Yeh Hsu: contributed to discussion.
Jyu-Gang Leu: investigated data.
Alexander Leemans: contributed to discussion, designed analysis, revised manuscript.

Acknowledgments

This work was sponsored by the Shin Kong Wu Ho-Su Memorial Hospital (SKH-8302-98-DR-19) and the project Care4Me (Cooperative Advanced REsearch for Medical Efficiency) in the framework of the EU research program ITEA (Information Technology for European Advancement).

References

Alexander, A.L., Hasan, K.M., Lazar, M., Tsuruda, J.S., Parker, D.L., 2001a. Analysis of partial volume effects in diffusion-tensor MRI. Magn. Reson. Med. 45, 770–780.
Alexander, D.C., Pierpaoli, C., Basser, P.J., Gee, J.C., 2001b. Spatial transformations of diffusion tensor magnetic resonance images. IEEE Trans. Med. Imaging 20, 1131–1139.
Ashburner, J., Friston, K.J., 2000. Voxel-based morphometry — the methods. Neuroimage 11, 805–821.
Ashburner, J., Friston, K.J., 2005. Unified segmentation. Neuroimage 26, 839–851.
Basser, P.J., Mattiello, J., LeBihan, D., 1994. MR diffusion tensor spectroscopy and imaging. Biophys. J. 66, 259–267.
Bastin, M.E., Munoz Maniega, S., Ferguson, K.J., Brown, L.J., Wardlaw, J.M., MacLullich, A.M., Clayden, J.D., 2010. Quantifying the effects of normal ageing on white matter structure using unsupervised tract shape modelling. Neuroimage 51, 1–10.

Beaulieu, C., 2002. The basis of anisotropic water diffusion in the nervous system — a technical review. NMR Biomed. 15, 435–455.

Biessels, G.J., Staekenborg, S., Brunner, E., Brayne, C., Scheltens, P., 2006. Risk of dementia in diabetes mellitus: a systematic review. Lancet Neurol. 5, 64–74.

Burgmans, S., van Boxtel, M.P., Gronenschild, E.H., Vuurman, E.F., Hofman, P., Uylings, H.B., Jolles, J., Raz, N., 2010. Multiple indicators of age-related differences in cerebral white matter and the modifying effects of hypertension. Neuroimage 49, 2083–2093.

Caeyenberghs, K., Leemans, A., Geurts, M., Taymans, T., Linden, C.V., Smits-Engelsman, B.C., Sunaert, S., Swinnen, S.P., 2010a. Brain–behavior relationships in young traumatic brain injury patients: DTI metrics are highly correlated with postural control. Hum. Brain Mapp. 31, 992–1002.

Caeyenberghs, K., Leemans, A., Geurts, M., Taymans, T., Vander Linden, C., Smits-Engelsman, B.C., Sunaert, S., Swinnen, S.P., 2010b. Brain–behavior relationships in young traumatic brain injury patients: fractional anisotropy measures are highly correlated with dynamic visuomotor tracking performance. Neuropsychologia 48, 1472–1482.

Carpenter, D.M., Tang, C.Y., Friedman, J.I., Hof, P.R., Stewart, D.G., Buchsbaum, M.S., Harvey, P.D., Gorman, J.G., Davis, K.L., 2008. Temporal characteristics of tract-specific anisotropy abnormalities in schizophrenia. Neuroreport 19, 1369–1372.

Chen, H.T., Lin, H.D., Won, J.G., Lee, C.H., Wu, S.C., Lin, J.D., Juan, L.Y., Ho, L.T., Tang, K.T., 2008. Cardiovascular autonomic neuropathy, autonomic symptoms and diabetic complications in 674 type 2 diabetes. Diabetes Res. Clin. Pract. 82, 282–290.

Della Nave, R., Foresti, S., Pratesi, A., Ginestroni, A., Inzitari, M., Salvadori, E., Giannelli, M., Diciotti, S., Inzitari, D., Mascalchi, M., 2007. Whole-brain histogram and voxel-based analyses of diffusion tensor imaging in patients with leukoaraiosis: correlation with motor and cognitive impairment. AJNR Am. J. Neuroradiol. 28, 1313–1319.

Eguchi, K., Kario, K., Shimada, K., 2003. Greater impact of coexistence of hypertension and diabetes on silent cerebral infarcts. Stroke 34, 2471–2474.

Folsom, A.R., Rasmussen, M.L., Chambless, L.E., Howard, G., Cooper, L.S., Schmidt, M.I., Heiss, G., 1999. Prospective associations of fasting insulin, body fat distribution, and diabetes with risk of ischemic stroke. The Atherosclerosis Risk in Communities (ARIC) Study Investigators. Diabetes Care 22, 1077–1083.

Gold, S.M., Dziobek, I., Sweat, V., Tirsi, A., Rogers, K., Bruehl, H., Tsui, W., Richardson, S., Javier, E., Convit, A., 2007. Hippocampal damage and memory impairments as possible early brain complications of type 2 diabetes. Diabetologia 50, 711–719.

Hernandez-Fonseca, J.P., Rincon, J., Pedreanez, A., Viera, N., Arcaya, J.L., Carrizo, E., Mosquera, J., 2009. Structural and ultrastructural analysis of cerebral cortex, cerebellum, and hypothalamus from diabetic rats. Exp. Diabetes Res. 2009, 329632.

Hsu, W.C., Chiu, Y.H., Chen, W.H., Chiu, H.C., Liou, H.H., Chen, T.H., 2007. Simplified electrodiagnostic criteria of diabetic polyneuropathy in field study (KCIS No. 14). Neuroepidemiology 28, 50–55.

Hsu, J.L., Leemans, A., Bai, C.H., Lee, C.H., Tsai, Y.F., Chiu, H.C., Chen, W.H., 2008. Gender differences and age-related white matter changes of the human brain: a diffusion tensor imaging study. Neuroimage 39, 566–577.

Hsu, J.L., Van Hecke, W., Bai, C.H., Lee, C.H., Tsai, Y.F., Chiu, H.C., Jaw, F.S., Hsu, C.Y., Leu, J.G., Chen, W.H., Leemans, A., 2010. Microstructural white matter changes in normal aging: a diffusion tensor imaging study with higher-order polynomial regression models. Neuroimage 49, 32–43.

Jones, D.K., Leemans, A., 2011. Diffusion tensor imaging. Methods Mol. Biol. 711, 127–144.

Jongen, C., van der Grond, J., Kappelle, L.J., Biessels, G.J., Viergever, M.A., Pluim, J.P., 2007. Automated measurement of brain and white matter lesion volume in type 2 diabetes mellitus. Diabetologia 50, 1509–1516.

Kobayashi, S., Okada, K., Koide, H., Bokura, H., Yamaguchi, S., 1997. Subcortical silent brain infarction as a risk factor for clinical stroke. Stroke 28, 1932–1939.

Kodl, C.T., Franc, D.T., Rao, J.P., Anderson, F.S., Thomas, W., Mueller, B.A., Lim, K.O., Seaquist, E.R., 2008. Diffusion tensor imaging identifies deficits in white matter microstructure in subjects with type 1 diabetes that correlate with reduced neurocognitive function. Diabetes 57, 3083–3089.

Lebel, C., Walker, L., Leemans, A., Phillips, L., Beaulieu, C., 2008. Microstructural maturation of the human brain from childhood to adulthood. Neuroimage 40, 1044–1055.

Leemans, A., Jones, D.K., 2009. The B-matrix must be rotated when correcting for subject motion in DTI data. Magn. Reson. Med. 61, 1336–1349.

Leemans, A., Sijbers, J., De Backer, S., Vandervliet, E., Parizel, P.M., 2005. Affine coregistration of diffusion tensor magnetic resonance images using mutual information. Lec. Notes Comput. Sci. 3708.

Leemans, A., Jeurissen, B., Sijbers, J., Jones, D.K., 2009. ExploreDTI: a graphical toolbox for processing, analyzing, and visualizing diffusion MR data. Proceedings of the 17th Annual Meeting of International Society for Magnetic Resonance in Medicine, Hawaii, USA, p. 3536.

Manschot, S.M., Brands, A.M., van der Grond, J., Kessels, R.P., Algra, A., Kappelle, L.J., Biessels, G.J., 2006. Brain magnetic resonance imaging correlates of impaired cognition in patients with type 2 diabetes. Diabetes 55, 1106–1113.

Musen, G., Lyoo, I.K., Sparks, C.R., Weinger, K., Hwang, J., Ryan, C.M., Jimerson, D.C., Hennen, J., Renshaw, P.F., Jacobson, A.M., 2006. Effects of type 1 diabetes on gray matter density as measured by voxel-based morphometry. Diabetes 55, 326–333.

Nichols, T.E., Holmes, A.P., 2002. Nonparametric permutation tests for functional neuroimaging: a primer with examples. Hum. Brain Mapp. 15, 1–25.

Novak, V., Last, D., Alsop, D.C., Abduljalil, A.M., Hu, K., Lepicovsky, L., Cavallerano, J., Lipsitz, L.A., 2006. Cerebral blood flow velocity and periventricular white matter hyperintensities in type 2 diabetes. Diabetes Care 29, 1529–1534.

Otsu, N., 1979. A threshold selection method from gray-level histograms. IEEE Trans. Syst. Man Cybern. 9, 62–66.

Patel, S.A., Hum, B.A., Gonzalez, C.F., Schwartzman, R.J., Faro, S.H., Mohamed, F.B., 2007. Application of voxelwise analysis in the detection of regions of reduced fractional anisotropy in multiple sclerosis patients. J. Magn. Reson. Imaging 26, 552–556.

Pierpaoli, C., Basser, P.J., 1996. Toward a quantitative assessment of diffusion anisotropy. Magn. Reson. Med. 36, 893–906.

Pierpaoli, C., Barnett, A., Pajevic, S., Chen, R., Penix, L.R., Virta, A., Basser, P., 2001. Water diffusion changes in Wallerian degeneration and their dependence on white matter architecture. Neuroimage 13, 1174–1185.

Sage, C.A., Van Hecke, W., Peeters, R., Sijbers, J., Robberecht, W., Parizel, P., Marchal, G., Leemans, A., Sunaert, S., 2009. Quantitative diffusion tensor imaging in amyotrophic lateral sclerosis: revisited. Hum. Brain Mapp. 30, 3657–3675.

Salat, D.H., Tuch, D.S., Greve, D.N., van der Kouwe, A.J., Hevelone, N.D., Zaleta, A.K., Rosen, B.R., Fischl, B., Corkin, S., Rosas, H.D., Dale, A.M., 2005. Age-related alterations in white matter microstructure measured by diffusion tensor imaging. Neurobiol. Aging 26, 1215–1227.

Smith, S.M., 2002. Fast robust automated brain extraction. Hum. Brain Mapp. 17, 143–155.

Song, S.K., Sun, S.W., Ramsbottom, M.J., Chang, C., Russell, J., Cross, A.H., 2002. Dysmyelination revealed through MRI as increased radial (but unchanged axial) diffusion of water. Neuroimage 17, 1429–1436.

Song, S.K., Sun, S.W., Ju, W.K., Lin, S.J., Cross, A.H., Neufeld, A.H., 2003. Diffusion tensor imaging detects and differentiates axon and myelin degeneration in mouse optic nerve after retinal ischemia. Neuroimage 20, 1714–1722.

Stahl, R., Dietrich, O., Teipel, S.J., Hampel, H., Reiser, M.F., Schoenberg, S.O., 2007. White matter damage in Alzheimer disease and mild cognitive impairment: assessment with diffusion-tensor MR imaging and parallel imaging techniques. Radiology 243, 483–492.

Sullivan, E.V., Pfefferbaum, A., 2007. Neuroradiological characterization of normal adult ageing. Br. J. Radiol. 80, S99–S108 Spec No 2.

Tournier, J.D., Mori, S., Leemans, A., 2011. Diffusion tensor imaging and beyond. Magn. Reson. Med. 65, 1532–1556.

van Harten, B., de Leeuw, F.E., Weinstein, H.C., Scheltens, P., Biessels, G.J., 2006. Brain imaging in patients with diabetes: a systematic review. Diabetes Care 29, 2539–2548.

Van Hecke, W., Leemans, A., D'Agostino, E., De Backer, S., Vandervliet, E., Parizel, P.M., Sijbers, J., 2007. Nonrigid coregistration of diffusion tensor images using a viscous fluid model and mutual information. IEEE Trans. Med. Imaging 26, 1598–1612.

Van Hecke, W., Leemans, A., Sijbers, J., Vandervliet, E., Van Goethem, J., Parizel, P.M., 2008a. A tracking-based diffusion tensor imaging segmentation method for the detection of diffusion-related changes of the cervical spinal cord with aging. J. Magn. Reson. Imaging 27, 978–991.

Van Hecke, W., Sijbers, J., D'Agostino, E., Maes, F., De Backer, S., Vandervliet, E., Parizel, P.M., Leemans, A., 2008b. On the construction of an inter-subject diffusion tensor magnetic resonance atlas of the healthy human brain. Neuroimage 43, 69–80.

Van Hecke, W., Nagels, G., Leemans, A., Vandervliet, E., Sijbers, J., Parizel, P.M., 2010. Correlation of cognitive dysfunction and diffusion tensor MRI measures in patients with mild and moderate multiple sclerosis. J. Magn. Reson. Imaging 31, 1492–1498.

Verhoeven, J.S., Sage, C.A., Leemans, A., Van Hecke, W., Callaert, D., Peeters, R., De Cock, P., Lagae, L., Sunaert, S., 2010. Construction of a stereotaxic DTI atlas with full diffusion tensor information for studying white matter maturation from childhood to adolescence using tractography-based segmentations. Hum. Brain Mapp. 31, 470–486.

Vos, S.B., Jones, D.K., Viergever, M.A., Leemans, A., 2011. Partial volume effect as a hidden covariate in DTI analyses. Neuroimage 55, 1566–1576.

Wahlund, L.O., Barkhof, F., Fazekas, F., Bronge, L., Augustin, M., Sjogren, M., Wallin, A., Ader, H., Leys, D., Pantoni, L., Pasquier, F., Erkinjuntti, T., Scheltens, P., 2001. A new rating scale for age-related white matter changes applicable to MRI and CT. Stroke 32, 1318–1322.

Wessels, A.M., Simsek, S., Remijnse, P.L., Veltman, D.J., Biessels, G.J., Barkhof, F., Scheltens, P., Snoek, F.J., Heine, R.J., Rombouts, S.A., 2006. Voxel-based morphometry demonstrates reduced grey matter density on brain MRI in patients with diabetic retinopathy. Diabetologia 49, 2474–2480.

Wheeler-Kingshott, C.A., Cercignani, M., 2009. About "axial" and "radial" diffusivities. Magn. Reson. Med. 61, 1255–1260.

Yau, P.L., Javier, D., Tsui, W., Sweat, V., Bruehl, H., Borod, J.C., Convit, A., 2009. Emotional and neutral declarative memory impairments and associated white matter microstructural abnormalities in adults with type 2 diabetes. Psychiatry Res. 174, 223–230.

Yau, P.L., Javier, D.C., Ryan, C.M., Tsui, W.H., Ardekani, B.A., Ten, S., Convit, A., 2010. Preliminary evidence for brain complications in obese adolescents with type 2 diabetes mellitus. Diabetologia 53, 2298–2306.